Brucella melitensis outer membrane protein 25 interacts with ferritin heavy polypeptide 1 in human trophoblast cells

YU ZHANG[1], XIAOFENG WANG[1], ZHIQIANG LI[2], JING ZHANG[1], YONG WANG[1],
CHANGXIN WU[3], CHUANGFU CHEN[1], JIE LI[1] and HUI ZHANG[1]

[1]College of Animal Science and Technology, Shihezi University, Shihezi, Xinjiang 832003;
[2]College of Biology and Food, Shangqiu Normal University, Shangqiu, Henan 476000;
[3]Institute of Biomedical Sciences, Shanxi University, Taiyuan, Shanxi 030006, P.R. China

Abstract. Outer membrane protein 25 (OMP25) is involved in *Brucella* virulence and serves an important role in *Brucella* pathogenesis during infection. However, the protein interacting with OMP25 in host cells remains to be elucidated. The present study constructed a cDNA library from *Brucella melitensis* 16M-infected human placenta trophoblastic cells (HPT-8) and identified and confirmed the interaction between *Brucella* OMP25 and ferritin heavy polypeptide 1 (FTH1) of HPT-8 using yeast two-hybrid and co-immunoprecipitation technologies. The expression of Toll-like receptor (TLR)4, myeloid differentiation primary response protein MyD88 (MyD88) mRNA and inflammatory factors was detected by RNA interference. The results showed that OMP25 interacted with FTH1. Subsequently, TLR4 and MyD88 mRNA expression levels and inflammatory factors, such as nitric oxide, lactate dehydrogenase and TNF-α, significantly increased after inserting OMP25 into the HPT-8 cells. Notably, a low dose of OMP25 resulted in immunological protection, whereas high dose of OMP25 resulted in a cytotoxic effect on the HPT-8 cells. It is suggested that OMP25 and FTH1 serve important roles in intracellular parasitism of *Brucella* and inhibition of expression.

Introduction

Brucella melitensis (*B. melitensis*) is a facultatively intracellular bacterium that causes brucellosis, which is a human zoonosis that can be transmitted though infected animals or contaminated food products. Brucellosis in humans and

Correspondence to: Professor Jie Li or Professor Hui Zhang, College of Animal Science and Technology, Shihezi University, 221 North 4th Road, Shihezi, Xinjiang 832003, P.R. China
E-mail: jieli2020@shzu.edu.cn
E-mail: allanzhh@sohu.com

animals can cause spontaneous abortion and diseases, such as endocarditis, arthritis, meningitis and osteomyelitis. This disease is a severe threat to human health and ruminant production, and results in economic loss worldwide (1-5).

Brucella has a small genome, but can invade the placental trophoblast cells (PTCs) of pregnant animals and subsequently result in placentitis and even spontaneous abortion (6). *Brucella*-infected PTCs have reportedly adapted to specific pathological changes, suggesting a unique pathogen-host relationship between *B. melitensis* and PTCs (7). PTCs are a link between mother and fetus and have an important role in maternal-fetal immunity (8). Dysfunction of PTCs may result in pregnancy-related diseases and *Brucella* interacts with PTCs and can cause infertility and spontaneous abortion (9). Thus, PTCs serve a key role in the immune system (10,11).

Bacterial outer membrane proteins (OMPs) can be easily recognized by the immune system, which produces antibodies or activates cellular immune responses (12). During infection, OMP25, a surface protein of *Brucella*, first establishes contact with host cells and completes the adhesion process (13). Studies have revealed that the OMP family is an important virulence factor of *Brucella* and that the virulence of *Brucella* is directly related to the uptake of iron (14-16); the pathogen efficiently uptakes iron and increases its virulence (17,18).

Ferritin heavy polypeptide 1 (FTH1) is involved in cell proliferation, immune response and iron homeostasis. Tsuji *et al* (19,20) reported that the upstream region of *FTH1* gene contains an antioxidant response element, which responds to oxidation reaction and protects cells from oxidative damage. Oxidative reaction may lead to apoptosis (21).

Trophoblasts are target cells of *Brucella* and there have been a number of studies on OMP25 in cell models, including human monocyte/macrophages, microglial cells and RAW264.7 mouse macrophages (22-24). However, few studies on OMP25 in human trophoblast cells have been reported. Therefore, the present study aimed to examine this interaction in HPT-8 cells.

To improve our understanding of the interaction between OMP25 of *B. melitensis* 16M strain and host FTH1 in human trophoblast cell line HPT-8, the present study investigated the related changes in the biological functions of *Brucella*-infected HPT-8 cells. In addition, the mRNA expression levels of

Toll-like receptor (TLR)4, myeloid differentiation primary response protein MyD88 (MyD88) and inflammatory factors, including nitric oxide (NO), lactate dehydrogenase (LDH) and TNF-α, in the OMP25-transfected HPT-8 cells were analyzed.

Materials and methods

Bacterial strains, plasmids and cell line. B. melitensis strain 16M strain was procured from the Chinese Center for Disease Control and Prevention (Beijing, China). *Brucella* was cultured in tryptic soy agar (TSA) or tryptic soy broth (both Sigma-Aldrich; Merck KGaA) without any antibiotics. *Brucella* was incubated in an atmosphere with 5% CO_2 at 37°C for 3 days. Subsequently, the cells were observed and counted. DH5α and BL21 strains of *Escherichia coli* (*E. coli*) were procured from Promega Corporation. The two strains were grown on Luria-Bertani medium (Beijing Solarbio Science & Technology Co., Ltd.). The culture medium was supplemented with antibiotics [100 µg/ml ampicillin or kanamycin (Invitrogen; Thermo Fisher Scientific, Inc.)] when necessary. Purification of OMP25 recombinant protein was performed as previously reported (24). pGBKT7, a plasmid, was procured from Promega Corporation. pMD18-T simple vector, another plasmid, was procured from Takara Bio, Inc. DNA ladder was procured from Takara Bio, Inc. The human trophoblast HPT-8 cell line was procured from Cell Resource Center (http://m.cellresource.cn/content.aspx) and was cultured in Dulbecco's modified Eagle's medium (DMEM, Gibco; Thermo Fisher Scientific, Inc.) supplemented with 10% fetal bovine serum (FBS, Gibco; Thermo Fisher Scientific, Inc.) at 37°C in an atmosphere with 5% CO_2 (vol/vol).

Construction of a cDNA library of HPT-8 cells infected with B. melitensis 16M strain. A cDNA library of HPT-8 cells infected with *B. melitensis* 16M strain was constructed as previously described (25). Briefly, the number of HPT-8 cells was determined using flow cytometry. Viable *B. melitensis* 16M strain was obtained by plating serially diluted colony-forming units on TSA after a 4 day-incubation at 37°C in an atmosphere with 5% CO_2. The HPT-8 cells were infected with the 16M strain at a dilution of 100:1 for 4 h at 37°C. The infected cells were incubated at 37°C in an atmosphere with 5% CO_2.

To validate infection efficiency, genomic DNA was separately prepared using a number of the infected cells ($1x10^5$/ml) using a DNeasy® Blood & Tissue kit (Qiagen GmbH), according to the manufacturer's protocols. OMP25-F and OMP25-R primers (Table I) were designed for the amplification of the *OMP25* gene.

To construct a cDNA library of HPT-8 cells, total RNA was separately prepared from the infected cells using TRIzol® (Thermo Fisher Scientific, Inc.) and Ultrapure RNA kit (CoWin Biosciences; cat. no. CW0597S), according to the manufacturer's protocols. HPT-8 cDNA library construction was performed according to Make Your Own 'Mate & Plate' Library System Protocol (Clontech Laboratories, Inc.) as previously described (26). The inserts of cDNA library were detected by long-distance PCR (LD-PCR) as previously described (26) with some modifications. The LD-PCR reaction conditions were as follows: 1 min at 95°C, followed by 40 cycles at 95°C for 15 sec, 68°C for 3 min.

Construction of the pGBKT7-OMP25 bait system. The open reading frame of OMP25 in the genome of *B. melitensis* 16M was amplified using OMP25-F and OMP25-R primers (Table I). The total PCR reaction volume was 15 µl, containing ddH_2O 13.9 µl, Up-primer (25 µM) 0.4 µl, Down-primer (25 µM) 0.4 µl, dNTP (2.5 mmol) 0.8 µl, 10x PCR Buffer 2.0 µl, Templet (genome of *B. melitensis* 16M) 2.0 µl, Taq DNA Polymerase (5 U/µl) 0.5 µl. The PCR reaction conditions were as follows: 5 min at 95°C, followed by 30 cycles at 94°C for 30 sec, 55°C for 45 sec and 72°C for 1 min, and 10 min at 72°C. The PCR product was cloned into pGBKT7 vector via *Eco*R I/*Xho* I sites, and to generate a recombinant plasmid: pGBKT7-*OMP25*. The recombinant pGBKT7-*OMP25* plasmid was transformed into the Y2HGold yeast strain.

Negative and positive controls of yeast two-hybrid system. Yeast two-hybrid test was performed, as previously described (27). Competent Y187 cells that were transformed with pGADT7-T from the Matchmaker™ Gold Yeast Two-Hybrid System (Clontech Laboratories, Inc.) was used as a control for the prey system and pGBKT7-53 and pGBKT7-Lam-transformed yeast Y187 cells were used as a positive and negative controls, respectively. Then, pre-two-hybrid experiments were then performed to test the positive and negative control systems.

Interactive screening of Y2HGold (pGBKT7-OMP25) and Y187 (pGADT7-cDNA) yeast strains. The pGBKT7-*OMP25*-containing yeast Y2HGold was inoculated into 50 ml SD/-Trp/Kan (Clontech Laboratories, Inc.) liquid medium (50 µg/ml) and cultured for 20 h at 30°C with shaking at 10.48 x g. The bacterial density was adjusted to $>10^9$/ml by a centrifugation at 1,000 x g at 30°C for 10 min. Yeast Y187 cells with a density of $>2x10^7$/ml stored at -80°C were thawed and yeast two-hybrid assays were performed using Matchmaker™ Gold Yeast Two-Hybrid System (Clontech Laboratories, Inc.). The resuspended yeast culture was spread onto 150 mm SD/-Ade/-His/-Leu/-Trp/X-α-Gal (QDO/X) plates (Clontech Laboratories, Inc.) that were inverted and incubated at 30°C for 72 h. Afterwards, the recombinant plasmids were extracted from the positive colonies that were identified by SD/-Ade/-His/-Leu/-Trp screening, PCR amplification and sequencing. The PCR reaction volume and conditions were described above.

Validation of the yeast two-hybrid results by co-immunoprecipitation (Co-IP). The pGBKT7-*OMP25* and positive plasmids identified by pGADT7-cDNA library screening were transcribed and translated using a TNT T7 polymerase-coupled reticulocyte lysate system (Promega Corporation). Briefly, the total reaction volume of TNT T7 transcription and translation was 25 µl, containing TNT Rabbit Reticulyte Lysate 12.5 µl, TNT Reaction Buffer 1 µl, Amino Acid Mixture Minus Leucine (1 mM) 0.5 µl, Amino Acid Mixture Minus Methionine (1 mM) 0.5 µl, Recombinant RNasin Ribonuclease Inhibitor (40 U/µl) 0.5 µl, DNA template 1.0 µl, Transcend tRNA 0.5 µl, Nuclease-Free Water 7.0 µl, TNT RNA Polymerase 0.5 µl. *In vitro* transcribed and translated bait and prey proteins (10 µl) were incubated at room temperature for 1 h. Then, 10 µl c-Myc monoclonal antibody (cat. no. MA1-980; Invitrogen; Thermo Fisher Scientific, Inc.)

Table I. Primers used in the present study.

Primer	5'-3' sequence
OMP25-F	Forward: GAATTCATGCGCACTCTTAAGTCTCTC
OMP25-R	Reverse: CTGCAGTTAGAACTTGTAGCCGATGCC
FTH1-F	Forward: GCAGGATATAAAGAAACCAGA
FTH1-R	Reverse: TCTCAATGAAGTCACATAAGT
16S rRNA-F	Forward: CACCCCGACGGCTAACATTCA
16S rRNA-R	Reverse: AGTGTAGAGGTGAAATTCGTA
GAPDH-F	Forward: GTCGTGGAGTCTACTGGTGT
GAPDH-R	Reverse: TGCTGACAATCTTGAGTGA
TLR4-F	Forward: CTTTAGACCTGTCCCTGAACC
TLR4-R	Reverse: CTAAACCAGCCAGACCTTGA
MyD88-F	Forward: CCTAACCATGTCCCTGAACA
MyD88-R	Reverse: GGTACATAATGGGTCCTTTCC

OMP25, outer membrane protein 25; FTH1, ferritin heavy polypeptide; TLR, Toll-like receptor; MyD88, myeloid differentiation primary response protein MyD88; F, forward; R, reverse.

was added to the protein mixture and the mixture was incubated at room temperature for another 1 h. Subsequently, the above samples were added to a centrifuge tube containing 3 μl Protein A bead (Matchmaker™ Co-IP kit, cat. no. 630449, Clontech Laboratories, Inc.) and incubated at room temperature for 1 h. Then 500 μl Buffer 1 was added and centrifuged at 350 x g for 30 sec at room temperature. The supernatant was discarded, 600 μl Buffer 2 added and centrifuged at 350 x g for 30 sec at room temperature and the supernatant discarded. The proteins were electrophoresed via SDS-PAGE on 12% gels and electrotransferred to a nitro-cellulose (NC) membrane using a Mini Trans-Blot Cell (Bio-Rad Laboratories, Inc.) at 200 mA for 1 h. The NC membrane was incubated in blocking solution [5% nonfat milk in Tris-buffered saline 0.05% Tween-20 (TBST)] for 1 h at room temperature. Then the membrane was incubated in binding buffer (6 μl Streptavidin-AP in 15 ml TBST) at room temperature for 1 h. After three washes with TBST, the membrane was stained with Western Blue Stabilized Substrate (Promega Corporation) at room temperature for 2-6 h. The signal was detected and densitometry performed by a Micro-Chemi instrument (GelView 6000Plus, Guangzhou Biolight Biotechnology Co., Ltd.).

Reverse transcription-quantitative (RT-q) PCR. The total RNA was separately prepared from the infected cells using TRIzol® (Thermo Fisher Scientific, Inc.) and Ultrapure RNA kit (CoWin Biosciences; cat. no. CW0597S), according to the manufacturer's protocols. cDNA was synthesized from the total RNA of the infected cells (1x10^5) using reverse transcription kit (cat. no. 639505; Takara Biotechnology Co., Ltd.) at 42˚C for 50 min and at 85˚C for 5 min, and was then used as a PCR template for amplification of *FTH1* and construction of pGM-T-A/B/C/D plasmids. The plasmids were extracted from the positive clones that were identified using PCR and considered a reference standard after determining the concentration of plasmids. Furthermore, the pGM-T-FTH1 plasmid was identified using *Eco*R I/*Xho* I digestion. Genes were amplified

as templates with pGM-T-FTH1 plasmid, 16M, GAPDH and HPT-8 cDNA with primers (Table I) designed for FTH1, 16S rRNA and reference gene GAPDH. RT-qPCR was performed according to Roche LightCycler® 480 (Roche Diagnostics, Switzerland) protocol; standard curves were generated based on the standard templates. SYBR Green I Master was used as fluorophore (Roche Diagnostics). The total RT-qPCR reaction volume was 10 μl, containing ddH$_2$O 3.6 μl, up-primer (10 μM) 0.2 μl, down-primer (10 μM) 0.2 μl, template 1.0 μl, SYBR Green I Master 5.0 μl. The thermocycling conditions were as follows: Preincubation for 5 min at 95˚C, and then 40 cycles of amplification (95˚C for 30 sec, 60˚C for 30 sec and 72˚C for 30 sec). The relative transcriptional levels were determined using the 2$^{-\Delta\Delta Cq}$ method (28). All assays were performed in triplicate and repeated at least three times.

Construction of pSIREN-siRNA vector targeting FTH1 gene. The human *FTH1* gene (NCBI Reference Sequence: NM_002032) was submitted to Ambion (Thermo Fisher Scientific, Inc.); three pairs of positive small interfering (si)RNA fragments were identified for the *FTH1* gene and a pair of siRNA fragments containing a different gene was considered the negative control (Table II). siRNA fragments were synthesized by Sangon Biotech Co., Ltd. pSIREN-siRNA expression vector with green fluorescent protein was constructed according to the RNAi-Ready pSIREN-RetroQ ZsGreen Vector kit (Clontech Laboratories, Inc.) protocol. The diluted siRNA fragment (antisense strand) concentration was 100 μmol/l and the PCR conditions were as follows: 95˚C for 30 sec, 72˚C for 2 min, 37˚C for 2 min and 25˚C for 2 min. Synthetic double strands were diluted to 0.5 μmol/l and 5 μl synthetic double strands were electrophoresed in 1% agarose gel containing ethidium bromide; the DNA fragments were ligated using RNAi-Ready pSIREN-RetroQ ZsGreen Vector at 16˚C overnight. Subsequently, the ligated product was transformed into competent *E. coli* DH5α cells for 16-18 h and sequenced by Sangon Biotech Co., Ltd., to identify the positive

Table II. Synthesized DNA sequences associated with siRNA.

Primer	5'-3' sequence
FTH1-A1	GATCCAAACTGATGAAGCTGCAGAACTTCAAGAGAGTTCTGCAGCTTCATCAGTTTTTTTTTTACGCGTG
FTH1-A2	AATTCACGCGTAAAAAAAAACTGATGAAGCTGCAGAACTCTCTTGAAGTTCTGCAGCTTCATCAGTTTG
FTH1-B1	GATCCAAAGAAACCAGACCGTGATGATTCAAGAGATCATCACGGTCTGGTTTCTTTTTTTTTTACGCGTG
FTH1-B2	AATTCACGCGTAAAAAAAAAGAAACCAGACCGTGATGATCTCTTGAATCATCACGGTCTGGTTTCTTTG
FTH1-C1	GATCCAATCAGTCACTACTGGAACTGTTCAAGAGACAGTTCCAGTAGTGACTGATTTTTTTTTACGCGTG
FTH1-C2	AATTCACGCGTAAAAAAAATCAGTCACTACTGGAACTCTCTTGAACAGTTCCAGTAGTGACTGATTG
FTH1-D1	GATCCAATTCGAATCTCGCTGACCAGTTCAAGAGACTGGTCAGCGAGATTCGAATTTTTTTTTACGCGTG
FTH1-D2	AATTCACGCGTAAAAAAAATTCGAATCTCGCTGACCAGTCTCTTGAACTGGTCAGCGAGATTCGAATTG

FTH1, ferritin heavy polypeptide; siRNA, small interfering RNA.

plasmids, and digested using *Mlu* I and named pSIREN-A/B/C/D. The plasmids were prepared using Endotoxin-Free Plasmid Highpure kit (Tiangen Biotech Co., Ltd.), according to the manufacturer's protocols.

Detection of pSIREN-siRNA interference effect. pSIREN-A/B/C/D plasmids were transfected into HTP-8 cells using a Lipofectamine® 2000 Transfection Reagent kit (cat. no. 11668030; Invitrogen Co., Ltd.), and pSIREN-D was used as the negative control. The transfected HPT-8 cells were cultured in an atmosphere with 5% CO_2 at 37°C for 48 h and HPT-8 containing green fluorescent protein were observed under a LSM510 confocal laser scanning microscope (Zeiss GmbH). Total RNA was extracted from the transfected HTP-8 cells using Ultrapure RNA kit (CoWin Biosciences, cat. no. CW0597S), according to the manufacturer's protocols. cDNA was synthesized using a first-strand cDNA synthesis kit (CoWin Biosciences, cat. no. CW0741), according to the manufacturer's protocols. The mRNA expression of *FTH1* gene was measured using RT-PCR as described above. The target gene detection value and the reference gene detection value were regarded as a correction value in evaluating the effect of each interfering plasmid and were statistically analyzed before and after transfection. The *FTH1* gene corresponding value/GAPDH detection value was used as a correction value and interference efficiency was calculated as follows: Interference efficiency (%)=(RNAi negative control group-RNAi test group)/RNAi negative control group x100% (29).

Determination of OMP25 concentration by Bradford protein assay. The determination of OMP25 concentration was performed using a protein assay kit (Shanghai Yeasen Biotechnology Co., Ltd.).

Expression levels of NO, TNF-α and LDH in HPT-8 cells transfected with OMP25. The expression levels of NO, TNF-α and LDH were measured as previously described (30). HPT-8 cells were used to evaluated the effects of NO, TNF-α and LDH activity. Briefly, $1x10^6$ cells/well were cultured in a 24-well plate for 24 h at 37°C and transfected with OMP25 at low doses (0.25, 0.5 and 1 µg/ml) or high doses (1, 5, 10, 20 and 40 µg/ml). A group without OMP25 was used as a control. Subsequently, 24 or 48 h post-transfection, the supernatant was centrifuged at 16,000 x g at room temperature for 15 min and collected, NO and TNF-α expression levels were determined using a ELISA kit (NO, cat. no. KGE001; TNF-α, cat. no. DTA00D; R&D Systems, Inc.) and LDH expression level was determined using LDH assay kit (cat. no. ab102526; Abcam, Inc.), according to the manufacturer's protocols.

Expression levels of NO and TNF-α following pEGFP-OMP25 plasmid and siRNA-c co-transfection. Monolayers of HPT-8 cells at a density of $1x10^6$ cells/well were cultured in a 6-well plate until the cells achieved ~60% confluence. pEGFP-*OMP25* (3 µg) and siRNA-c (0, 2.5, 5, or 10 µl) were co-transfected into HPT-8 cells using Lipofectamine® 2000 reagent (Invitrogen; Thermo Fisher Scientific, Inc.) according to the manufacturer's protocol. At 48 h post-transfection, the supernatant was centrifuged at 16,000 x g at room temperature for 15 min and collected, and the expression levels of NO and TNF-α were measured as described above.

RT-qPCR for detection of TLR4 and MyD88 mRNA levels. To determine the mRNA levels of TLR4 and MyD88, the genes of TLR4 and MyD88 were cloned into pMD18-T simple vector. The standard curves of RT-qPCR were constructed using the
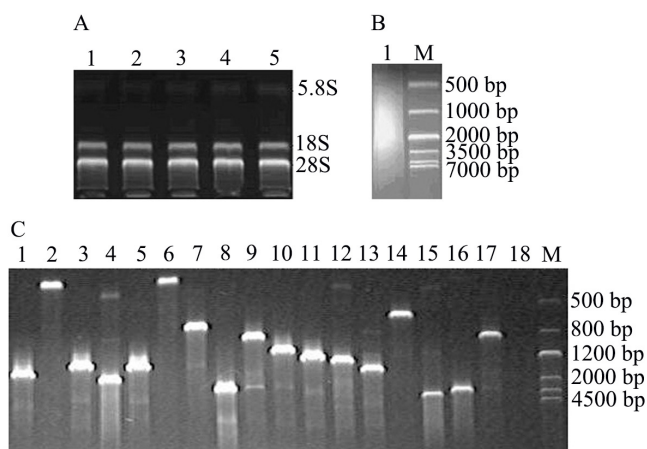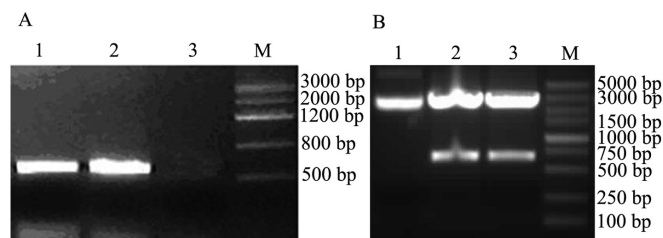
Figure 2. Identification of plasmid pGBKT7-OMP25. (A) Identification of plasmid pGBKT7-OMP25 by PCR. Lanes 1-2: PCR productions; Lane M: DNA Marker. (B) Identification of plasmid pGBKT7-OMP25 by restriction endonuclease digestion. Lane 1: pGBKT7-OMP25 plasmid control; Lanes 2-3: Products of plasmid pGBKT7-OMP25 with *Eco*R I/*Xho* I digestion; Lane M: DNA Marker.
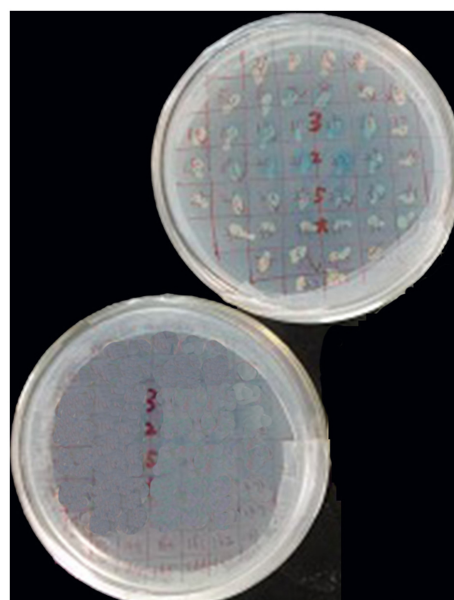
Figure 1. Assay of infected HPT-8 cells cDNA Library. (A) Total RNA in the HPT-8 cells. Lanes 1-5: HPT-8 cells were infected with *Brucella* at 20 min, 1-3 and 4 h, respectively. (B) Assay of LD-PCR productions. Lane 1: LD-PCR productions; Lane M: DNA Marker. (C) Inserts of cDNA library. Lanes 1-17: clones of cDNA library; Lane 18: negative control; Lane M: DNA Marker. LD-PCR, long-distance PCR.

primers TLR4-S, TLR4-A, MyD88-S and MyD88-A (Table I). RT-qPCR was performed as described above to measure TLR4 and MyD88 mRNA levels and the results were normalized against the standard curves.

Statistical analysis. The statistical differences between the groups were analyzed using one-way analysis of variance (ANOVA) followed by Tukey's post hoc test. The expression levels of NO, TNF-α and LDH are presented as the mean ± standard deviation. The differences between groups were analyzed using ANOVA in SPSS 17.0 software (SPSS, Inc.). $P < 0.05$ was considered to indicate a statistically significant difference. The experiments were repeated three times.

Results

Detection of infected HPT-8 cells. Three bands corresponding to 28S, 18S and 5.8S rRNA in the total RNA extracts were observed (Fig. 1A). The A260/280 value was 1.90 (20 min post-infection), 2.02 (1 h post-infection), 1.92 (2 h post-infection), 1.85 (3 h post-infection) and 2.04 (4 h post-infection), indicating the high purity of the total RNA. The library capacity of the cDNA was 1.43×10^6 transformants; thereby reaching the construction requirements. The cDNA library was also uncontaminated. The size of the cDNA insert fragments were mainly in the range of 0.2-5 kb and with the majority near the 1-2 kb region (Fig. 1B and C).

Yeast two-hybrid assay. DNA fragments of 640 bp size obtained using PCR and restriction enzyme digestion indicated that the target was the plasmid pGBKT7-*OMP25*. Y2HGold containing pGBKT7-*OMP25* had no self-activation or toxicity for cells (Fig. 2A and B).

Control assay. Blue colonies (2-3 mm) on the SD/-Ade/-His/-Leu/-Trp/X-α-Gal plates with Y187 (pGADT7-T) that matched Y2HGold (pGBKT7-53) as positive control were observed. No colonies were grown

Figure 3. Yeast two hybrid negative and positive control system.

on the SD/-Ade/-His/-Leu/-Trp/X-α-Gal plates with Y187 (pGADT7-T) that matched Y2HGold (pGBKT7-lam) as negative control (Fig. 3).

Interaction between prey protein and OMP25 bait protein. Colonies of 2-3 mm on SD/-Ade/-His/-Leu/-Trp plates with Y2HGold (pGBKT7-*OMP25*) matched Y187 (pGADT7-library) and these colonies switched to SD/-Ade/-His/-Leu/-Trp/X-α-Gal changed into blue colonies and were considered the positive colonies (Fig. 4). The OMP25 bait protein gene trap sequence of the prey protein gene was analyzed and the results indicated that the pGBKT7-*OMP25* bait plasmid eventually yielded seven positive AD plasmids. Blast analysis results are shown in Table III.

Verification of the interaction between prey protein and OMP25 by Co-IP. OMP25 carrying c-myc tag and *FTH1* carrying HA tag, were amplified with templates as pGBKT7-*OMP25* and pGADT7-prey (*FTH1* gene) using Advantage 2 PCR kit protocol (Fig. 5). The Co-IP results indicated that OMP25 interacted with FTH1.

Table III. Blast analysis result of AD plasmid.

| Gene	GenBank (Accession no.)
Hypothetical protein LOC789060	NM_001110188
NADH dehydrogenase 1 α subcomplex	NM_175826
Ribonucleoprotein, PTB-binding 1 mRNA	NM_001103108
Eyes absent homolog 2 mRNA	NM_001035464
Histone deacetylase 5 mRNA	NM_001038025
Solute carrier family 3	NM_001024488
Similar to Steroid hormone receptor ERR1	XM_001790466
Tryptophanyl-tRNA synthetase mRNA	BC102806
Insulin-like growth factor binding protein 6 mRNA	NM_001040495
Amidohydrolase domain containing 2 mRNA	NM_001101104
Actin, β mRNA	BC142413
Ancient ubiquitous protein 1 mRNA	BC102888
Haloacid dehalogenase-like hydrolase domain containing	BC102640
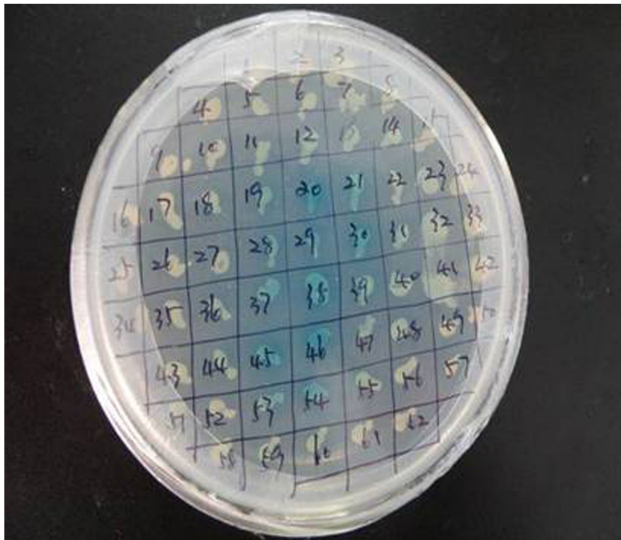
Figure 4. Positive screening of OMP25 bait protein. There were colonies (2-3 mm) on SD/-Ade/-His/-Leu/-Trp plates with Y2HGold (pGBKT7-*OMP25*) matching with Y187 (pGADT7-library), on switching to SD/-Ade/-His/-Leu/-Trp/X-α-Gal these colonies changed blue and were regarded as positive colonies. OMP25, outer membrane protein 25.

Figure 5. Advantage 2 PCR product for FTH1 and OMP25. Lane 1: FTH1 was obtained from pGADT7-prey; Lane 2: OMP25 was obtained from pG-BKT7-OMP25; Lane 3: Negative control; Lane M: DNA Marker. FTH1, ferritin heavy polypeptide; OMP25, outer membrane protein 25.

Bio-function of the interaction between FTH1 and OMP25 during brucellosis. The obtained *FTH1* gene ligated into pGM-T vector generated a positive plasmid: pGM-*FTH1*; which was identified using *Eco*R I/*Xho* I digestion and target fragment indicated a 550 bp band (Fig. 6A).

The results of the green fluorescent protein expression vector pSIREN-siRNA transfection indicated that a 69 bp positive fragment was inserted into Linearized pSIREN Vector and was sequenced (Fig. 6B); the sequencing results indicated that four small fragments of DNA sequences were identical with sequences in the original sequence.

The RT-qPCR detection results of *Brucella* survival ability in the transfected cells indicated that the relative expression of 16S rRNA decreased by ~84% in HPT-8 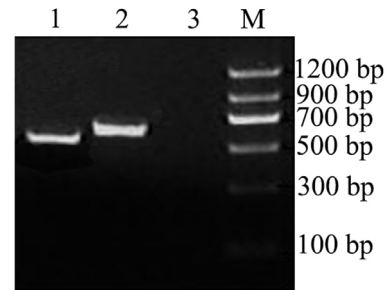cells containing interference plasmid vs. empty HPT-8 cells infected with *Brucella*; the viability of *brucella* was decreased in the host cells transfected with *FTH1* interference fragment.

HPT-8 cells were transfected and subsequently observed under a LSM 510 Laser scanning confocal microscope 48 h post-transfection. The results indicated green fluorescence protein expression in HPT-8 cells and a ~100% plasmid transfection efficiency was achieved (Fig. 5C-a and C-b).

The interference effect of four RNAi plasmids, namely pSIREN-A, pSIREN-B, pSIREN-C and pSIREN-D on the *FTH1* gene were detected, respectively. pSIREN-A, pSIREN-B and pSIREN-C interference plasmids exerted interference effects and an interference efficiency of ≤98% was achieved for pSIREN-C (Table IV).

NO, TNF-α and LDH activity in HPT-8 cells treated with OMP25 and siRNA-a. Low doses of OMP25 affected HPT-8 cells after 24 h and the levels of NO and TNF-α were positively associated with the concentration of OMP25 (Fig. 7A-a and -b). High doses of OMP25 affected HPT-8 cells after 24 h and the levels of NO and LDH were increased with the concentration of OMP25 (Fig. 7B-a and -b). Different doses of siRNA-a were transfected into HPT-8 cells and the levels of NO and LDH were decreased with the concentration of siRNA-a (Fig. 7C-a and C-b).

Table IV. Optimal siRNA plasmid screening.

Detection value	pSIREN-A	pSIREN-B	pSIREN-C	Negative
GAPDH average Cq value (x)	22.92	26.90	25.36	30.38
GAPDH copies (10^y)	11,081,537.00	1,475,707.00	3,219,586.00	253,162.90
FTH1 average Cq value (x)	24.69	30.38	31.90	29.50
FTH1 copies (10^y)	3,939,671.00	120,759.10	47,599.24	207,014.10
Inhibition ratio for FTH1 (%) [a]	57%	89%	98%	-

siRNA, small interfering RNA; FTH1, ferritin heavy polypeptide. [a]The FTH1 gene corresponding value/GAPDH detection value was used as a correction value and interference efficiency was calculated as follows: Interference efficiency (%)=(RNAi negative control group-RNAi test group)/RNAi negative control group x100%.
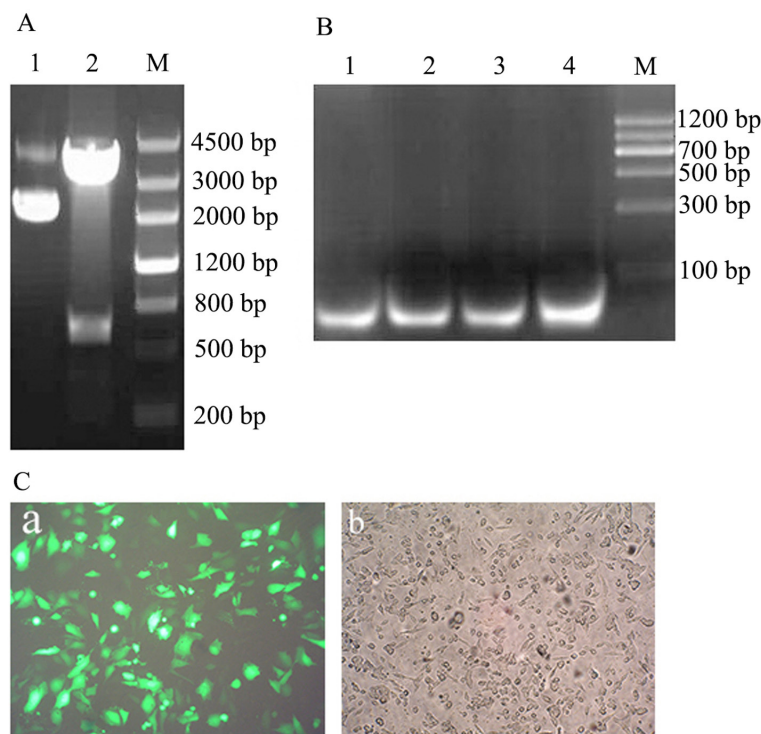

Figure 6. Biofunction of the interaction between FTH1 and OMP25. (A) PCR assay of pGM-T-FTH1. Lane 1: pGM-T-FTH1 plasmid; Lane 2: *Eco*R I/*Xho* I digestion of pGM-T-FTH1; Lane M: DNA Marker. (B) Double stranded DNA of siRNA DNA fragments. Lanes 1-4: siRNA DNA; Lane M: DNA Marker. (C) Fluorescence of the HPT-8 cells transfected with pSIREN-siRNA expression plasmids; (C-a) Transfected cell (48 h; magnification, x400) and (C-b) Control (magnification, x400). The green fluorescence protein expression in HPT-8 cells and the plasmid transfection efficiency achieved ~100%. FTH1, ferritin heavy polypeptide; OMP25, outer membrane protein 25; siRNA, small interfering RNA.

TLR4 and MyD88 mRNAs levels in HPT-8 cells treated with OMP25 protein and siRNA-c. Low doses of OMP25 affected HPT-8 cells and the relative expression levels of TLR4 and MyD88 were associated with the concentration of OMP25 (Fig. 8A). No significant differences observed for TLR4 (Fig. 8A).

siRNA-c and pGEFP-*OMP25* were co-transfected into HPT-8 cells and the relative expression levels of TLR4 were decreased with the increase of the concentration of siRNA-c (Fig. 8B).

Discussion

B. melitensis can efficiently invade trophoblast cells in mammals and rapidly multiply within the placenta, which can result in spontaneous abortion and placentitis (24,25). Trophoblast cells are therefore the primary target cells of *B. melitensis* in the infected host; however, the infection of trophoblast cells remain poorly understood. Spontaneous abortion in pregnant women resulting from brucellosis may indicate that if *Brucella* can reach the placenta and enter trophoblasts (27,30), they may also become an important cellular niche. *In vitro* studies regarding intracellular trafficking are few. The present study successfully obtained a cDNA library from HPT-8 cell lines infected with *B. melitensis* strain 16M and demonstrated that the protein OMP25 directly interacts with eukaryotic proteins such as FTH1, suggesting that OMP25 is a functional protein involved in the alteration of host cell processes. The interactions between
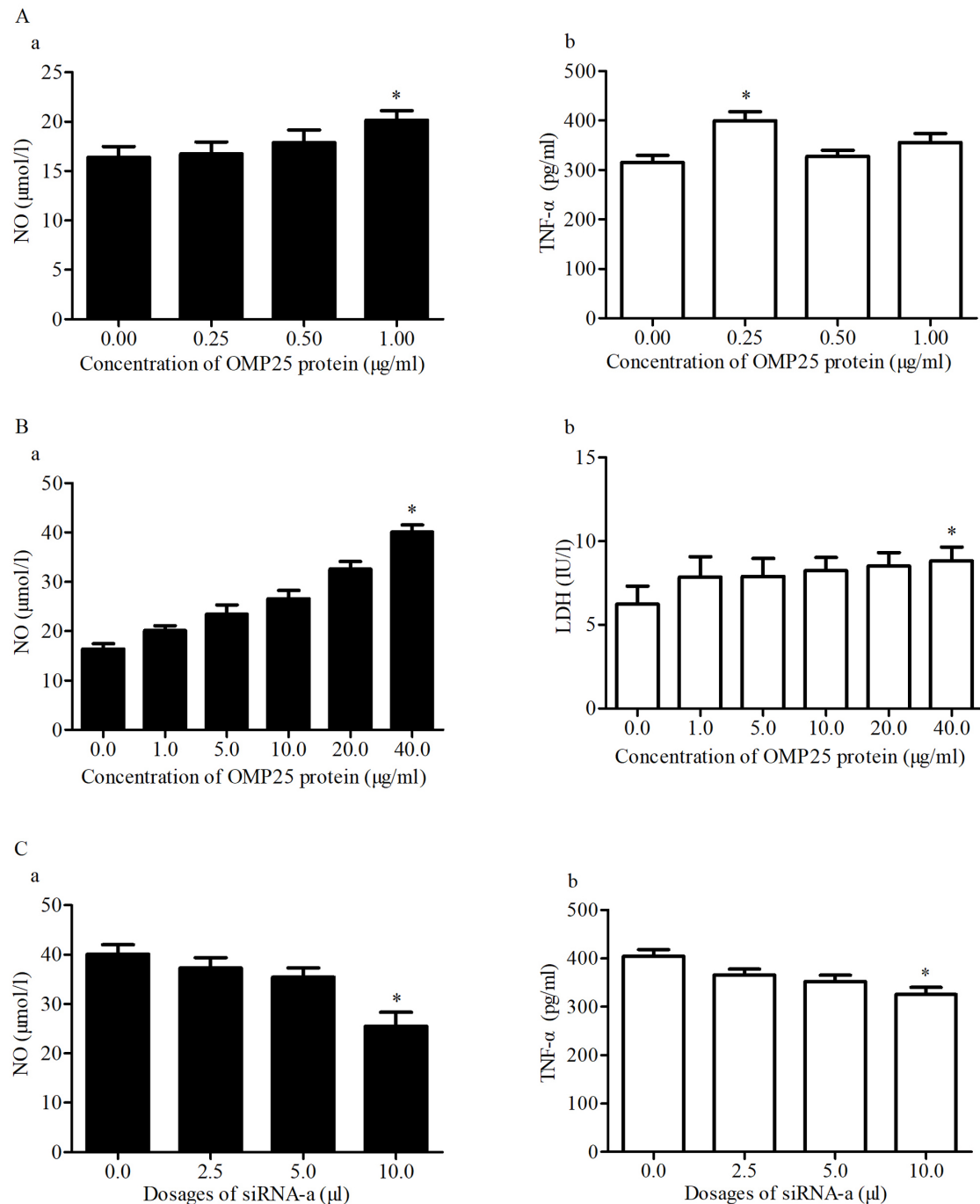
Figure 7. Cytokine levels in HPT-8 cells. (A-a) NO and (A-b) TNF-α in HPT-8 cells treated with OMP25 protein. Low doses of OMP25 affected HPT-8 cells after 24 h and the levels of NO and TNF-α were increased with the concentration of OMP25. (B-a) NO and (B-b) LDH in HPT-8 cells treated with the OMP25 protein. High doses of OMP25 affected HPT-8 cells after 24 h and the levels of NO and LDH were positively associated with the concentration of OMP25. (C-a) NO and (C-b) TNF-α in HPT-8 cells treated with siRNA-a. NO and LDH levels were negatively associated with the concentration of siRNA-a. Each experiment was repeated at least three times. *P<0.05 vs. 0 dose group. NO, nitric oxide; OMP25, outer membrane protein 25; LDH, lactate dehydrogenase; siRNA, small interfering RNA.

B. melitensis protein and host proteins *in vivo* further indicated that *Brucella* protein OMP25 serves an important role in the modulation of host cells via protein-protein or protein-DNA interactions.

B. melitensis OMP25 is a virulence protein involved in intracellular replication. LDH, an intracellular enzyme, is released into the extracellular matrix when cells are damaged or undergo death; this results in an increase in LDH activity in cell supernatants. In addition, LDH is considered an index for

cell injury (31). OMP25 at concentrations >5 µg/ml resulted in increased amounts of LDH in HPT-8 cells.

TLR is expressed on the surface of epithelial cells and is important to bacterial infection. The present study found that TLR4 mRNA was lowly expressed in the HPT-8 cells, whereas a low concentration of OMP25 upregulated TLR4 and inflammatory signaling molecules, including TNF-α and NO, in the HPT-8 cells. The activation of TLR4, MyD88, TNF-α and NO resulted in the activation of the nuclear transcription factor
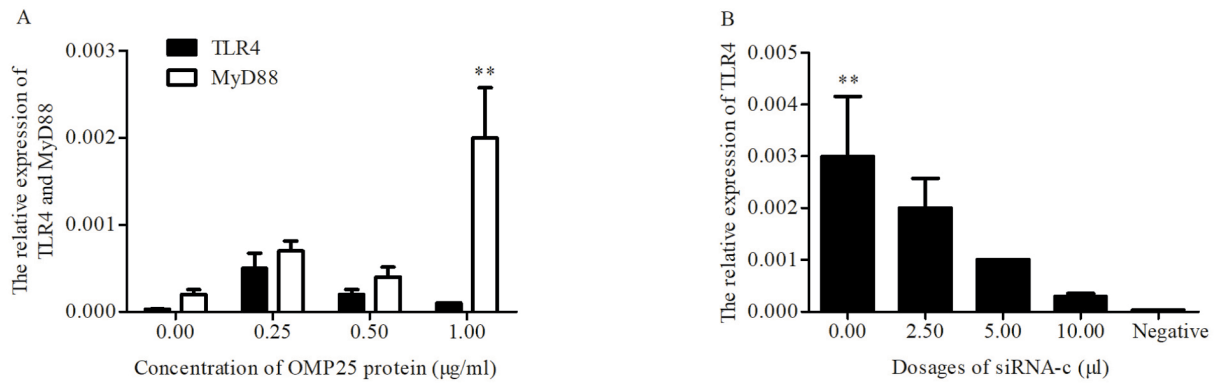
Figure 8. TLR4 and MyD88 mRNAs levels in HPT-8 cells treated with OMP25 protein and siRNA-c. (A) RT-qPCR analyses of TLR4 and MyD88 levels in the HPT-8 cells treated with OMP25 protein. The relative expression levels of TLR4 and MyD88 were associated with the concentration of OMP25. **P<0.01 vs. 0.00 μg/ml OMP25 group. (B) RT-qPCR analysis of TLR4 mRNA in the HPT-8 cells transfected with different concentrations of siRNA-c. The relative expression levels of TLR4 were negatively associated with the concentration of siRNA-c. Each experiment was repeated at least three times. **P<0.01 vs. negative control. TLR4, Toll-like receptor 4; MyD88, myeloid differentiation primary response protein MyD88; OMP25, outer membrane protein 25; siRNA, small interfering RNA; RT-qPCR, reverse transcription-quantitative PCR.

NF-κB, which may serve a key regulatory role in a variety of inflammatory responses in host cells.

In a previous study (32), we found that OMP25 serves an important role in the activation of the MAPK signaling pathway in HPT-8 cells infected with *Brucella*. 2308ΔOmp25 mutant strain could not activate p38 phosphorylation protein, ERK and JNK branches in HPT-8 cells. However, in the present study, it was found that OMP25 interacts with FTH1 in HPT-8 cells. The present study provided a theoretical basis regarding the new functions of OMP25.

The present study focused on the interaction between OMP25 and key molecules of trophoblast cells. Further studies, including on cell and animal experiments, are required to confirm whether OMP25 can help in the infection of trophoblast cells. The present study did not prove that OMP25 can help trophoblast infection and this is one of its limitations.

In conclusion, the results of the present study indicated that OMP25 interacts with FTH1. The mRNA expression levels of TLR4, MyD88 and inflammatory factors, including NO, LDH and TNF-α significantly increased after the interaction of OMP25 and FTH1 in the HPT-8 cells. OMP25-FTH1 interaction may contribute to the exacerbation of the intracellular replication of *Brucella* and the likelihood of a subsequent abortion or stillbirth of the infected fetus. Further research is required to elucidate the mechanisms underlying the molecular interactions of OMP25 with the host, such that other *Brucella* effector proteins and host cell targets can be identified to further elucidate and define the molecular mechanisms of brucellosis. Furthermore, the present study clarified the pathogenic mechanism of brucellosis and may yield novel insights for the development of therapeutic options.

Acknowledgements

Availability of data and materials

The datasets used and/or analyzed during the current study are available from the corresponding author on reasonable request.

Authors' contributions

HZ, ZL, CC, CW and JL contributed to the conception and design of the experiment. HZ, XW, ZL, JZ, YZ and YW performed all experiments and verified the analytical data. JZ, YZ and YW contributed to the statistical analysis and helped interpret the results. HZ supervised the experiments in discussion with ZL. JZ, YZ and YW wrote the manuscript. JL and HZ confirm the authenticity of all the raw data. All authors discussed the final results and all authors read and approved the final manuscript.

Ethics approval and consent to participate

Not applicable.

Patient consent for publication

Not applicable.

Competing interests

The authors declare that they have no competing interests.

References

1. Purwar S, Metgud SC, Karadesai SG, Nagamoti MB, Darshan A and Tiwari S: Triad of infective endocarditis, splenic abscess, and septicemia caused by *Brucella melitensis*. J Lab Physicians 9: 340-342, 2017.
2. Asmare K: Neospora caninum versus *Brucella* spp. exposure among dairy cattle in Ethiopia: A case control study. Trop Anim Health Prod 46: 961-966, 2014.
3. Cash-Goldwasser S, Maze MJ, Rubach MP, Biggs HM, Stoddard RA, Sharples KJ, Halliday JEB, Cleaveland S, Shand MC, Mmbaga BT, *et al*: Risk factors for human brucellosis in Northern Tanzania. Am J Trop Med Hyg 98: 598-606, 2018.
4. Bayasgalan C, Chultemdorj T, Roth F, Zinsstag J, Hattendorf J, Badmaa B, Argamjav B and Schelling E: Risk factors of brucellosis seropositivity in bactrian camels of Mongolia. BMC Vet Res 14: 342, 2018.
5. El-Sayed A and Awad W: Brucellosis: Evolution and expected comeback. Int J Vet Sci Med 6 (Suppl 1): S31-S35, 2018.
6. Meador VP and Deyoe BL: Intracellular localization of *Brucella* abortus in bovine placenta. Vet Pathol 26: 513-515, 1989.
7. Zhang J, Li M, Li Z, Shi J, Zhang Y, Deng X, Liu L, Wang Z, Qi Y and Zhang H: Deletion of the type IV secretion system effector VceA promotes autophagy and inhibits apoptosis in *Brucella*-Infected human trophoblast cells. Curr Microbiol 76: 510-519, 2019.
8. von Bargen K, Gorvel JP and Salcedo SP: Internal affairs: Investigating the *Brucella* intracellular lifestyle. FEMS Microbiol Rev 36: 533-562, 2012.
9. Anderson TD and Cheville NF: Ultrastructural morphometric analysis of *Brucella* abortus-infected trophoblasts in experimental placentitis. Bacterial replication occurs in rough endoplasmic reticulum. Am J Pathol 124: 226-237, 1986.
10. Sidhu-Muñoz RS, Sancho P and Vizcaíno N: Evaluation of human trophoblasts and ovine testis cell lines for the study of the intracellular pathogen *Brucella* ovis. FEMS Microbiol Lett 365, 2018.
11. Watanabe K, Tachibana M, Tanaka S, Furuoka H, Horiuchi M, Suzuki H and Watarai M: Heat shock cognate protein 70 contributes to *Brucella* invasion into trophoblast giant cells that cause infectious abortion. BMC Microbiol 8: 212, 2008.
12. Vassen V, Valotteau C, Feuillie C, Formosa-Dague C, Dufrêne YF and De Bolle X: Localized incorporation of outer membrane components in the pathogen *Brucella* abortus. EMBO J 38: e100323, 2019.
13. Degos C, Hysenaj L, Gonzalez-Espinoza G, Arce-Gorvel V, Gagnaire A, Papadopoulos A, Pasquevich KA, Méresse S, Cassataro J, Mémet S and Gorvel JP: Omp25-dependent engagement of SLAMF1 by *Brucella* abortus in dendritic cells limits acute inflammation and favours bacterial persistence in vivo. Cell Microbiol 22: e13164, 2020.
14. Cloeckaert A, Jacques I, Grilló MJ, Marín CM, Grayon M, Blasco JM and Verger JM: Development and evaluation as vaccines in mice of *Brucella melitensis* Rev.1 single and double deletion mutants of the bp26 and omp31 genes coding for antigens of diagnostic significance in ovine brucellosis. Vaccine 22: 2827-2835, 2004.
15. Paul S, Peddayelachagiri BV, Nagaraj S, Kingston JJ and Batra HV: Recombinant outer membrane protein 25c from *Brucella* abortus induces Th1 and Th2 mediated protection against *Brucella* abortus infection in mouse model. Mol Immunol 99: 9-18, 2018.
16. Basaraba RJ, Bielefeldt-Ohmann H, Eschelbach EK, Reisenhauer C, Tolnay AE, Taraba LC, Shanley CA, Smith EA, Bedwell CL, Chlipala EA and Orme IM: Increased expression of host iron-binding proteins precedes iron accumulation and calcification of primary lung lesions in experimental tuberculosis in the guinea pig. Tuberculosis (Edinb) 88: 69-79, 2008.
17. Rossi MS, Fetherston JD, Letoffe S, Carniel E, Perry RD and Ghigo JM: Identification and characterization of the hemophore-dependent heme acquisition system of Yersinia pestis. Infect Immun 69: 6707-6717, 2001.
18. Hop HT, Arayan LT, Huy TXN, Reyes AWB, Baek EJ, Min W, Lee HJ, Rhee MH, Watanabe K, Chang HH and Kim S: Lipocalin 2 (Lcn2) interferes with iron uptake by *Brucella* abortus and dampens immunoregulation during infection of RAW 264.7 macrophages. Cell Microbiol 20, 2018.
19. Tsuji Y: JunD activates transcription of the human ferritin H gene through an antioxidant response element during oxidative stress. Oncogene 24: 7567-7578, 2005.
20. Tsuji Y, Moran E, Torti SV and Torti FM: Transcriptional regulation of the mouse ferritin H gene. Involvement of p300/CBP adaptor proteins in FER-1 enhancer activity. J Biol Chem 274: 7501-7507, 1999.
21. Qian ZM, Li H, Sun H and Ho K: Targeted drug delivery via the transferrin receptor-mediated endocytosis pathway. Pharmacol Rev 54: 561-587, 2002.
22. Cui B, Liu W, Wang X, Chen Y, Du Q, Zhao X, Zhang H, Liu SL, Tong D and Huang Y: *Brucella* Omp25 upregulates miR-155, miR-21-5p, and miR-23b to inhibit interleukin-12 production via modulation of programmed death-1 signaling in human monocyte/macrophages. Front Immunol 8: 708, 2017.
23. Ma QL, Liu AC, Ma XJ, Wang YB, Hou YT and Wang ZH: *Brucella* outer membrane protein Omp25 induces microglial cells in vitro to secrete inflammatory cytokines and inhibit apoptosis. Int J Clin Exp Med 8: 17530-17535, 2015.
24. Zhang J, Guo F, Huang X, Chen C, Liu R, Zhang H, Wang Y, Yin S and Li Z: A novel Omp25-binding peptide screened by phage display can inhibit *Brucella* abortus 2308 infection in vitro and in vivo. J Med Microbiol 63: 780-787, 2014.
25. Jiang H, Dong H, Peng X, Feng Y, Zhu L, Niu K, Peng Y, Fan H and Ding J: Transcriptome analysis of gene expression profiling of infected macrophages between *Brucella* suis 1330 and live attenuated vaccine strain S2 displays mechanistic implication for regulation of virulence. Microb Pathog 119: 241-247, 2018.
26. Yang YJ, Liu ZS, Lu SY, Li C, Hu P, Li YS, Liu NN, Tang F, Xu YM, Zhang JH, *et al*: Molecular cloning, expression and characterization of programmed cell death 10 from sheep (ovis aries). Gene 558: 65-74, 2015.
27. Berta P, Bourg G, Hanna N, Saadeh B, Armengaud J, Patey G and O'Callaghan D: The *Brucella* suis IbpA heat-shock chaperone is not required for virulence or for expression of the VirB type IV secretion system VirB8 protein. Lett Appl Microbiol 58: 564-568, 2014.
28. Livak KJ and Schmittgen TD: Analysis of relative gene expression data using real-time quantitative PCR and the 2(-Delta Delta C(T)) method. Methods 25: 402-408, 2001.
29. Guo F, Wang Y, Chen C, Zhang H, Qiao J, Ren Y, Zhang J and Li Z: Interaction between VirB5 of *Brucella* type IV secretion system (TFSS) and ferritin heavy polypeptide 1 (FTH1) in murine macrophage. J Anim Vet Adv 11: 2623-2629, 2012.
30. Zhang Y, Li T, Zhang J, Li Z, Zhang Y, Wang Z, Feng H, Wang Y, Chen C and Zhang H: The *Brucella melitensis* M5-90 phosphoglucomutase (PGM) mutant is attenuated and confers protection against wild-type challenge in BALB/c mice. World J Microbiol 32: 58, 2016.
31. Meng L, Ma H, Meng J, Li T, Zhu Y and Zhao Q: Costunolide attenuates oxygen-glucose deprivation/reperfusion-induced mitochondrial-mediated apoptosis in PC12 cells. Mol Med Rep 23: 411, 2021.
32. Zhang J, Zhang Y, Li Z, Liu J, Shao X, Wu C, Wang Y, Wang K, Li T, Liu L, *et al*: Outer membrane protein 25 of *Brucella* activates mitogen-activated protein kinase signal pathway in human trophoblast cells. Front Vet Sci 4: 197, 2017.